J. Fluid Mech. (1974), *vol.* **62**, *part* 1, *pp.* 11–31
Printed in Great Britain

Turbulent vortex streets and the entrainment mechanism of the turbulent wake

By DEMOSTHENES D. PAPAILIOU† AND PAUL S. LYKOUDIS

School of Aeronautics, Astronautics and Engineering Sciences,
Purdue University

(Received 30 August 1972 and in revised form 9 April 1973)

The results of an experimental investigation of a turbulent vortex street in the range $10^3 \lesssim Re \lesssim 2 \times 10^4$ are presented. The vortex street was created by the motion of a circular cylinder in a motionless fluid (mercury). Photographs obtained showed that the turbulent street, created by the vortex shedding behind the cylinder, persisted at longer downstream distances and higher Reynolds numbers than previously reported in the literature. A theory was developed to account for the experimental measurements pertaining to the change of the geometrical characteristics, h (distance between the two rows of vortices) and α (longitudinal distance between two consecutive vortices on the same row), of the street in the downstream direction. The implications of the structure of the vortex street on the entrainment mechanism of the turbulent wake are discussed. Some observations of the flow in the formation region of the vortices are discussed in relation to existing work.

1. Introduction

Strouhal (1878) first observed the periodic shedding of vortices behind a bluff body moving in a fluid, and the subsequent downstream formation of a vortex street. Although the phenomenon has been the subject of both experimental and theoretical investigations for almost a century, it is far from being understood. On the contrary, features reported during the last twenty years have revealed many difficulties (see e.g. Rosenhead 1953; Marris 1964; Morkovin 1964; Berger & Wille 1972).

The subject is important because of its association with wake flows and the initiation of turbulence, its role in structural problems, and its participation in aerodynamic sound phenomena. Also, interest in vortex flows has lately been renewed, because of their relation to atmospheric phenomena and aeroplane flying.

The basic questions associated with the problem concern the mechanism of vortex formation behind the moving body and the subsequent periodic shedding in the near wake region, the geometry of the vortex street and its change in the downstream direction, the mechanism by which vorticity decays in the street and the mechanism of transition of the flow in the wake into turbulence. It can

† Present address: Propulsion Research and Advanced Concepts Section, Jet Propulsion Laboratories, Pasadena, California.

be said that our understanding of the phenomena pertaining to the above questions is presently in a state of change, and it resembles an unfinished puzzle with only certain pieces placed together. Our knowledge on the subject can be summarized as follows.

Above a Reynolds number of about 40, the vortex street occurs behind the moving body. In the range $40 \lesssim Re \lesssim 200$, where the vortex street is stable and laminar, two different mechanisms of vortex formation and shedding have been identified. As Kovasznay (1949) observed, the vortices are formed by an instability which develops downstream within the laminar wake. This was verified by Tritton (1959, 1971), who also reported a change of mode at $Re \simeq 90$. In the range $90 \lesssim Re \lesssim 150$–$300$, the vortices are shed near the cylinder, and are produced by a 'double vortex sheet' laminar instability (Tritton 1959, 1971; Marris 1964; Morkovin 1964), resulting in an alteration of the longitudinal spacing of the vortices in the street. The results of Tritton were confirmed by Berger (1964*a*, *b*), who also investigated the effect of free-stream turbulence on the appearance of the two modes. However, Gaster (1969, 1971) questioned the above observations, attributing the appearance of the two different modes of vortex formation to non-uniformities existing in the oncoming flow.

At Reynolds numbers covering the range of about 200 up to the critical value of 10^5, a 'single vortex sheet' instability develops in each of the free vortex layers originating on the cylinder. This instability results in the rolling-up of each vortex layer and the periodic formation of secondary vortices (Mattingly 1962; Morkovin 1964). Further downstream, a 'double vortex sheet' instability is created and dominates the flow.

The significance of the interaction between the two layers of opposite vorticity in the development of the 'double vortex sheet' instability was demonstrated experimentally first by Roshko (1954) for the case of a cylinder. By inserting a splitter plate at an appropriate location in the near wake region of the body, he was able to change the frequency and finally completely suppress the vortex formation due to the 'double vortex sheet' instability.

At Reynolds numbers between the critical value of about 10^5, where the reattachment of the two vortex layers occurs, and the value $3{\cdot}5 \times 10^6$, a complete loss of periodicity has been observed (Humphreys 1960; Morkovin 1964). Above $Re = 3{\cdot}5 \times 10^6$, Roshko (1961), who performed experiments up to Reynolds numbers of approximately 10^7, found a recovery of the periodicity in the near wake, possibly caused by the same 'double sheet' instability. Roshko's results were confirmed by Jones, Cincotta & Walker (1969), who found that the periodic vortex shedding reappears at Reynolds numbers between 6×10^6 and 10×10^6.

Transition to turbulence occurs in the flow at Reynolds numbers above 200, its location in the wake depending on the Reynolds number. Studies on transition were conducted by Schiller & Linke (1933), Roshko (1953), Bloor (1964), Gerrard (1965, 1966*a*) and other investigators. Roshko (1953), in an experimental study of the development of the wake behind cylinders, detected the initiation of turbulent motions in the free vortex layers at $150 < Re < 300$. Beyond this range, according to his observation, the wake is turbulent, the periodic shedding persists but the vortices are quickly obliterated by the action

of turbulent diffusion. Spectral analysis of the u component of the velocity showed no trace of periodicity beyond 40–50 diameters downstream.

Schiller & Linke (1933) made the observation (verified by Bloor 1964) that, as the Reynolds number increases from approximately 10^3 to about 10^4, transition to turbulence moves towards the cylinder, while the vortex formation region reduces in size.

The geometry of the vortex street was first considered by von Kármán & Rubach (1912), who examined the stability of two infinite rows of potential vortices. Domm (1956) proved that the von Kármán street configuration is unstable to second-order perturbations. At the moment, the use of hydrodynamic stability theory as a tool for the investigation of the geometry of the vortex street for either an inviscid or a viscous fluid is being seriously questioned (Wille 1966), because it can take into account neither the finite length of the street nor the different rates of ageing of the vortices in it.

The broadening of the vortex street in the downstream direction owing to the action of viscosity was the subject of several experimental and theoretical investigations. It has been observed experimentally that the ratio h/α changes in the downstream direction. As Hooker (1936) suggested, the real centre of the vortex (i.e. the point of maximum vorticity) does not coincide with the apparent centre of the vortex (i.e. the point of zero velocity). The use of Hooker's definition of vortex position revealed that both the distance h and longitudinal spacing α change in the downstream direction (Wille & Timme 1957), though the change in the latter is much smaller. Frimberger (1957), who applied hot-wire anemometry to measure the geometrical characteristics of the vortex street, reports that in the range of $1{\cdot}5 \times 10^3 \lesssim Re \lesssim 1{\cdot}4 \times 10^4$ the longitudinal spacing α increases at a distance of about 8 cylinder diameters. The velocity of translation initially decreases in the downstream direction, reaches a minimum at the same distance of 8 cylinder diameters and subsequently increases to a constant value of about $0{\cdot}20\ U_0$.

Theoretical studies of the effect of viscosity on the geometry of the vortex street, besides the work of Domm (1955), who examined the change with time of the vortex street in which the line vortices were replaced with vortices subjected to the effect of viscosity, are those of Birkhoff (Birkhoff 1952; Birkhoff & Zarantanello 1957) and Lin (1954). Birkhoff introduced a 'main invariance' theorem, according to which the moment of vorticity k^*h (where k^* is the mean vorticity per unit length) for a finite or infinite vortex street remains constant. The work of Lin will be discussed in more detail in what follows, since the model proposed in his theory is used and extended in this work.

Taneda (1959) reported experimental observations concerning the downstream development of vortex streets behind cylinders and flat plates. The experiments with cylinders covered the range $10 \lesssim Re \lesssim 10^3$. These observations showed that, in both the laminar ($Re \lesssim 150$) and turbulent ($Re \gtrsim 150$) flow regimes, a repeated breakdown and rebirth of the vortex street occurs. After each breakdown the laminar or turbulent wake rearranged itself into a new von Kármán vortex street of larger wavenumber. In the laminar case, the breakdown of the primary street was followed by an immediate appearance of the secondary

vortex street. By contrast, in the turbulent case the appearance of the secondary vortex street was delayed for a considerable downstream distance, after the breakdown of the primary street into turbulence. It was also found that the wavenumber ratio of the secondary to the primary turbulent streets was much larger than that observed in the laminar case.

The experimental findings of Taneda will be discussed later in this work in relation to the present observations.

2. Description of the experiment

The initial purpose of conducting the present experiment was to study the effect of a magnetic field on the shedding mechanism and the geometry of the von Kármán vortex street.† To obtain a strong interaction of the flow with the magnetic field, the working fluid was mercury. The vortex street was produced by the uniform traverse of a Plexiglas cylinder through the motionless mercury. Because of the low kinematic viscosity of mercury, the minimum Reynolds number attained (corresponding to the lowest values of the cylinder's diameter and traverse velocity used in the experiment) was about 750. This prohibited experimentation in the range of Reynolds numbers corresponding to stable laminar vortex streets ($40 \lesssim Re \lesssim 200$), as was initially planned. However, the limitation proved advantageous in producing high Reynolds numbers for relatively small velocities (compared, for instance, with corresponding velocities required to produce the same Reynolds numbers in water). The slow flow motion, combined with the long exposure time applied in obtaining photographs of the flow pattern, made possible the observation and study of the structure of the turbulent vortex street within a wide range of Reynolds numbers

$$(10^3 \lesssim Re \lesssim 2 \times 10^4).$$

The significance of the duration of exposure time in obtaining the detailed structure of the vortex street was evident in some of the photographs taken at low Reynolds numbers, in which shorter than 1 s exposure times were used. In those photographs (exposure time $\frac{1}{4}$ or $\frac{1}{8}$ s), only the part close to the cylinder where vortices are strong appears (see figure 6, plate 5), while photographs taken under approximately the same conditions, but with a 1 s exposure time, showed the existence of vortices far downstream. This proves also that the vortices are not frozen circular streamlines due to a previous alignment of the tracer particles,‡ but that they possess rotational motion. The mercury was contained in a tray 2030 mm long by 177 mm wide and 50 mm deep. The part of the cylinder immersed in the mercury was about 40 mm. The tray was placed in the gap between the horizontally positioned pole faces of the rotating electromagnet of the magneto-fluid-mechanics laboratory.

† The results obtained in the presence of a magnetic field will be reported in another paper.

‡ This pattern was actually observed when a high magnetic field was applied in the flow. There, the vortices appear 'frozen', and could be observed as regular vortex patterns without a real motion.

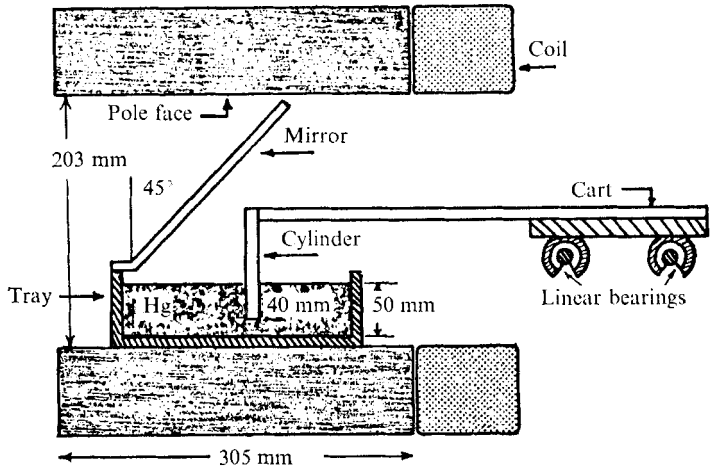

FIGURE 1. Experimental set up.

d (mm)	l/d	w/d
3·17	12·50	56
6·35	6·30	28
9·52	4·20	19
16·00	2·50	11

TABLE 1

The choice of the dimensions of the tray was dictated by space restrictions due to the geometry of the pole faces of the magnet, as shown in figure 1. This imposed certain limitations on the cylinder's aspect ratio l/d (l is the length of the cylinder) and the ratio w/d of the width of the channel to the diameter of the cylinder. The values of the ratios l/d and w/d, for the various cylinders used in the experiments, are shown in table 1. Side-wall confinement, although not well investigated, has been recognized as a factor influencing the character of the flow in the oscillating wake behind bluff bodies. Experiments, such as those conducted by Mattingly (1962) and Keefe (1961) at high Reynolds numbers, showed that confinement at the two ends of a cylinder by planes normal to the axis of the cylinder resulted in an increased two-dimensionality in the flow behind the cylinder. In the case of towing-tank experiments, where there are no boundary layers near the top or the bottom of the moving body, effects of the ending of the moving body can influence the flow in its close vicinity. However, it is accepted from experience that results obtained with aspect ratios $l/d > 5$ can adequately represent the flow behind cylinders of infinite length (Berger & Wille 1972). At low Reynolds numbers, Shair *et al.* (1963) found that the stabilizing effect of the confining walls resulted in an increase of the critical Reynolds number at which the von Kármán street was formed. Taneda (1955) concluded, from experiments with moving cylinders in water, that side-wall effects are negligible for ratios w/d above 50, although he did not describe the observations leading to this conclusion.

The above discussion indicates that some of the conclusions of the present work, especially those obtained with the largest cylinder, might not apply in the case of an unbounded wake.

The vertical moving cylinder was attached to an aluminium arm, the other end of which was bolted to an aluminium cart, as shown in figure 1. The cart rode on a system of linear bearings attached to its underside, over a track consisting of two polished stainless-steel cylindrical rods. The two rods were supported at their ends. The motion of the cart was determined by a system consisting of a cable and a number of pulleys properly connected to a d.c. synchronous motor of adjustable r.p.m. All moving parts and the two rods were carefully aligned to provide a smooth, continuous motion of the cart.

The velocity of the cylinders ranged from about 3 to 15 cm s^{-1}, covering the range of Reynolds numbers from 10^3 to about 2×10^4. Repeated measurements showed that the velocity of the cylinder was constant within less than 1 %.

The study of the vortex street, consisting of measuring the previously defined geometrical characteristics h and α, as well as the shedding frequency of the vortices, was made by using photography and hot-film anemometry.

The visualization of the vortex street was accomplished by spreading lycopodium powder on the surface of the mercury. The photographic method used in this experiment, which is common in the study of vortex streets in liquids (see, for instance, Timme 1957; Wille 1960), presented certain problems, owing to the use of mercury as the working fluid. The free surface of the mercury very rapidly forms a mercury oxide coating, which prevents visualization of the flow pattern. Therefore, the oxide had to be removed mechanically shortly before each trial. This created motions in the fluid which could distort the vortex flow and required several hours to damp out; and during this time a new coat of mercury oxide would form. Fortunately, it was possible to damp completely these motions in the fluid by applying a magnetic field of approximately 6000 Gauss for about 5 min before each trial.

The photographs were taken through a mirror attached to one side of the tray, its reflecting surface forming a 45° angle with the free surface of the mercury, as shown in figure 1. The 45° angle arrangement of the mirror eliminated any directional distortion of the image of the street. This was also checked by taking photographs of a thin Plexiglas strip placed on the mercury surface, on which lines were drawn with ink to form a net of 10×10 mm squares.

The camera used was a Nikon F Model with f 1·4 Nikor lens. A Nikon F 36 motor driving mechanism, operated by remote control, was attached to the camera, permitting consecutive photographs of the street to be obtained. The exposure time was $\frac{1}{8}$–1 s, depending on the Reynolds number, to allow the particles to trace a measurable path.

The hot-film sensor was attached to the same aluminium arm as the cylinder, thus moving with it. Its location with respect to the cylinder was ten diameters downstream, 1·5 diameters off the centre-line, and immersed in the mercury at a depth corresponding to about half the cylinder's length. All hot-film signals were taken behind the cylinder with $d = 6{\cdot}35$ mm.

From the study of the photographs the distances h and α, as functions of the

downstream distance x from the centre of the cylinder, were obtained,† while the shedding frequency of the vortices was measured from the signals of the hot-film sensor. Also, from consecutive photographs of the street, the translational velocity u_T of identified single vortices was measured.

3. Discussion of the experimental results

The study of the photographs of the turbulent vortex street, obtained with an exposure time of 1 s, suggests the following qualitative description pertaining to its structure.

In the range $10^3 \lesssim Re \lesssim 5{\cdot}5 \times 10^3$ the wake consists of two rows of turbulent vortices travelling at the edges of a turbulent core (figures 2, 3; plates 1, 2). Because of the turbulent action, the flow pattern is irregular, and at many points the vortices are scattered, deformed or completely disintegrated. The breakdown of vortices is observed in several photographs, and can be described as follows. The vortex breaks into smaller rotating parts, which initially remain within the vortex (figure 4(*b*), plate 3). Subsequently, those parts separate, forming smaller lumps of rotating turbulent fluid (figures 3, 5; plates 2, 4).

The scatter and breakdown of the vortices increases with the downstream distance from the moving cylinder (figure 4(*b*), plate 3) and Reynolds number; however, the vortex street persists, in the sense that vortices, which have been identified as being shed by the cylinder, are found in a more or less regular pattern far downstream, at distances at which it was generally accepted that they should have been completely obliterated and lost their identity. This persistence is present in all photographs.

The downstream distances covered in the photographs range from about 300 diameters for $Re = 1080$ and 1730 to approximately 180 diameters in the case of $Re = 5215$ (figures 2, 3; plates 1, 2).‡ No observation was made to establish the maximum distance from the cylinder at which the discussed flow pattern persists.

An approximately symmetric distribution of the vortices appears in most of the obtained photographs. Although this symmetry could be attributed to the existence of small vibrations of the cylinder (Taneda 1965; Berger & Wille 1972), observation of the early part of the vortex street shows that initially the vortices are shed alternately, forming the regular von Kármán street. This can be seen in figures 4(*b*), 9, 10 (plates 3, 8, 9), and was observed in several photographs not shown here. This symmetry appears to be the result of distortion of the wave form of the oscillatory motion occurring in the core of the street, and the displacement of vortices, some of which are seen to be located at the crests of the wave form (figures 2, 3, 4; plates 1, 2, 3). The symmetrical orientation of the vortices is most often observed after the broadening of the core due to the turbulent action (see arrows in figures 9, 10; plates 8, 9). This indicates that

† In defining the location of the vortices, the apparent centre of vorticity (point of zero velocity) was used.

‡ Besides the representative cases shown in figures 2, 3 (plates 1, 2), photographs of the street were taken at Reynolds numbers 1330, 1950 and 2620 (cylinder diameter = 3·175 mm) and also 1950, 2650, 3900 and 5480 (cylinder diameter = 6·35 mm). All photographs show the same general structure of the wake as figures 2, 3 (plates 1, 2).

turbulent motions in the street might be responsible for this structure, although no detailed mechanism is available at present to explain the observation.

At Reynolds numbers above approximately $5{\cdot}5 \times 10^3$, the structure of the turbulent wake changes, as can be seen in figures 4–6 (plates 3–5). A strong oscillatory motion appears in the wake, while the vortices continue to persist up to about the Reynolds number of 2×10^4 which marks the upper limit of the present investigation. The distances covered in the photographs in the case of $Re \gtrsim 5{\cdot}5 \times 10^3$ are between 60 and 80 diameters (figures 5, 6; plates 4, 5). Here again, no attempt was made to define either the downstream distance or the upper limit of Reynolds number at which the flow pattern under discussion ceases to occur. However, it is clear that the vortices persist within the region Townsend (1956) (see also Hinze 1959) found the overall structure of the turbulent wake to be self-preserving ($x/d \simeq 90$). Townsend's results also indicate that, for the detailed turbulent structure of the wake, self-preservation occurs at distances beyond $x/d = 1000$. It is possible that self-preservation is related to the vortex pattern observed in the present work and its influence on the structure of turbulence in the wake.

The breakdown and subsequent rebirth of the vortex street, found by Taneda at lower Reynolds numbers ($Re \lesssim 10^3$), is not observed in the present experiments, at least to the extent reported by Taneda. At lower Reynolds numbers (figures 2, 3, 4(*a*); plates 1, 2, 3), the vortex street is preserved at large downstream distances, although scatter and breakdown of individual vortices is observed at some points. At higher Reynolds numbers, regions such as those appearing at the right side of figure 5 (plate 4) indicate considerable deterioration of order in the street. Hot-wire measurements in these regions can lead to the conclusion drawn by Roshko (1953), concerning the disappearance of periodicity in the wake. However, here again the complete breakdown 'for considerable downstream distances' and subsequent rebirth of the vortex street, reported by Taneda, is not observed. The organized vortex motion is not completely lost in these regions, and the vortices can be identified as those shed by the cylinder. A satisfactory explanation of the observed differences between the present experiments and those of Taneda at lower Reynolds numbers is not evident, although some possibilities will now be discussed.

The effect of confining walls on the vortex street was discussed in § 2. It should be noted that, according to Taneda (1955), at least in the case of the smaller cylinder ($w/d = 56$, $l/d = 12{\cdot}5$), the flow should be free from wall effects. It is possible though that, as the street broadens rapidly in the downstream direction, the vortices could experience the stabilizing effects of the side walls.

Use of inadequate exposure times in Taneda's experiments could also explain part of the observed differences. For instance, relatively short exposure time could prevent weak vortices, existing in flow regions similar to that shown in figure 5 (plate 4), from appearing in the photograph. Unfortunately no information is given on the exposure time used in Taneda's work. Preliminary results from experiments conducted in a water tank,† to examine the effect of wall confine-

† The authors are indebted to Mr D. Irvine, who conducted these experiments at the Aerospace Sciences Laboratories of Purdue University.

ment on the street, showed the existence of vortices in the wake only when an exposure time of 2 s was used. The water tank was 4170 mm long, 915 mm wide and 254 mm deep. The diameter of the cylinder was 9·52 mm, corresponding to the ratios $w/d = 96$ and $l/d = 20$. A characteristic photograph of the structure of the wake at $Re = 3300$ is shown in figure 11 (plate 10). The photograph shows vortices at approximately 460 diameters downstream of the moving cylinder. This indicates that, at least for $Re < 3300$, the organized vortex motion observed in mercury is not the result of wall effects. However, the origin of the vortices cannot be inferred from this observation since only a small part of the wake is shown in the photograph. A systematic investigation of the entire wake, presently under progress, is expected to show whether the vortices belong to the primary or secondary vortex street.

The formation of the vortex street will now be discussed, to relate the present observations to previous work.

The 1 s exposure time prohibited visualization of the flow existing within the distance traversed by the moving cylinder during exposure. Depending on the speed and the diameter of the cylinder, this distance varied between 6 and 30 diameters. To investigate the near wake region, the exposure time was reduced to $\frac{1}{8}$ or $\frac{1}{4}$ s. Photographs taken this way show the formation region of the street in the two cases previously discussed, corresponding to $Re \lesssim 5{\cdot}5 \times 10^3$ and $Re \gtrsim 5{\cdot}5 \times 10^3$. The flow pattern in the formation region, shown in figure 7 (plate 6), appears to correspond to the case of low free-stream disturbances, discussed by Gerrard (1965, 1967) in relation to the minimal lift values measured on the cylinder in his experiments (1961, 1965). The observed symmetry in the flow, seen in this photograph, confirms that in this range of Reynolds numbers the two vortex layers develop independently in the formation region, as suggested by Gerrard. The secondary vortices, formed very close to the cylinder by the action of the 'single vortex street' instability (Mattingly 1962; Morkovin 1964) which develops within each vortex layer, are also shown in this photograph (also in figure 8, plate 7). The symmetrical arrangement of the secondary vortices might be due to small vibrations of the moving cylinder. At the end of the formation region the 'double vortex sheet' instability develops, producing the two rows of vortices of the von Kármán street.

At higher Reynolds numbers (figure 8, plate 7) a strong interaction of the two layers occurs, producing the oscillatory motion observed in this case in the far wake. A comparison with the experimental measurements of the oscillating velocity at the side of the cylinder made by Gerrard (1961, 1965) shows that the amplitude of this quantity starts increasing in the range $Re \simeq 5{\cdot}5 \times 10^3$, at which the change of mode in the formation region was observed in the present experiments. It is also interesting to note the resemblance of the flow patterns observed in this work to the flow in the formation region shown in Gerrard (1967, figures 13, 15), corresponding to Reynolds numbers 2×10^3 and 3×10^4.

The formation length was measured from figures 7, 8 (plates 6, 7), corresponding to Reynolds numbers $3{\cdot}4 \times 10^3$ and $1{\cdot}9 \times 10^4$. The point at which the outside fluid first crosses the axis of the wake was considered to be the end of the formation region, as suggested by Gerrard (1966*b*). The values $3{\cdot}1d$ and $2{\cdot}2d$

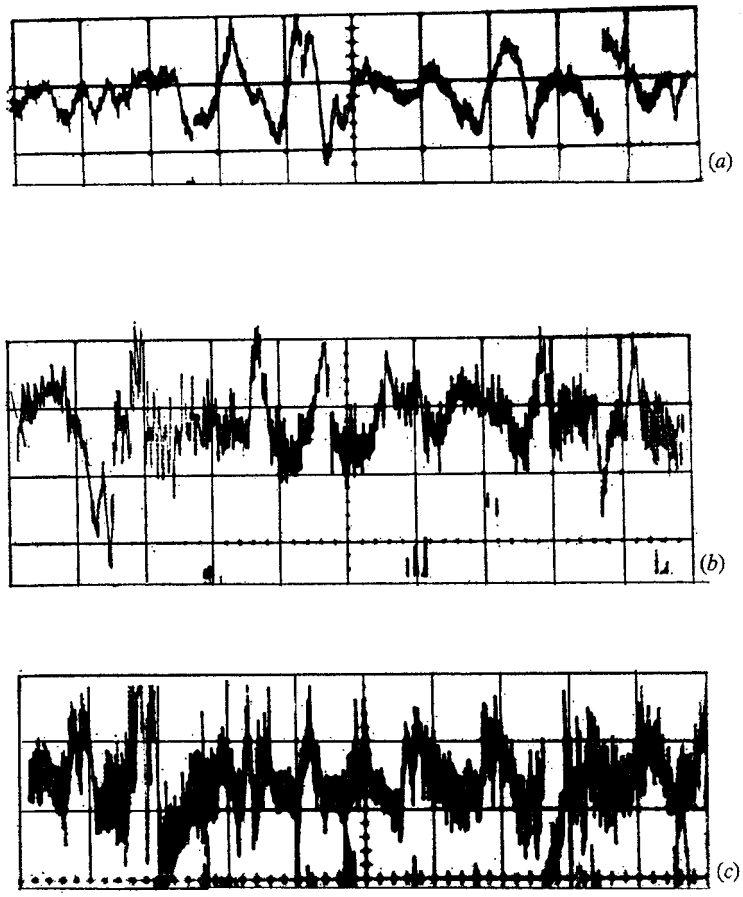

FIGURE 12. Shedding frequency of the vortices as it appears in the hot-film signals.

	Re	t (s div^{-1})	f approx. (vortices s^{-1})	Strouhal no.
(*a*)	2656	0·5	1·67	0·22
(*b*)	3900	0·4	2·15	0·2
(*c*)	5200	0·4	2·9	0·2

were obtained for the lower and higher Reynolds numbers, respectively. In the case of higher Reynolds numbers, the position of the moving cylinder could not be determined accurately; thus, the value $2{\cdot}2d$ for the formation length should be considered approximate. In both cases, the values obtained are slightly higher than those measured by Bloor for the case interpreted by Gerrard (1966*b*) as corresponding to low free-stream turbulence. As suggested by Gerrard (1966*b*), the formation region should shrink with increasing free-stream turbulence, to smaller sizes corresponding to higher Reynolds numbers. Therefore, the complete absence of disturbances in the fluid in the present experiment is expected to result in an increase of the formation length, as compared with that measured by Bloor at the same Reynolds numbers.

The signals obtained from the hot-film sensor were very irregular owing to the turbulent motions in the flow. After filtering the signal, the periodic oscillation corresponding to the expected shedding frequencies appeared (figure 12). The

filtering process was as follows. The signal from the hot-film sensor was recorded with the aid of a 7600 Honeywell tape-recorder. The recording speed was either 15 i.p.s. or 30 i.p.s. The tape was then played back at higher speeds (30 i.p.s. and 120 i.p.s.). This shifted the spectrum of the recorded frequencies to higher values, and made it possible to reduce the turbulent level in the signal by passing it through a low-pass filter (50 cycles).

At low Reynolds numbers ($Re \lesssim 5{\cdot}5 \times 10^3$) the oscillatory motion associated with the 'double vortex sheet' instability loses strength very soon after the appearance of turbulence in the flow. In this case, the turbulent motion pushes the vortices to the edges of the wake, thus leading to the formation of the turbulent core at the centre-line. At Reynolds numbers higher than $5{\cdot}5 \times 10^3$ the 'double vortex sheet' instability was very powerful, being able to overcome the diffusive turbulent action and develop downstream.

A careful observation of the photographs reveals that, at Reynolds numbers above $5{\cdot}5 \times 10^3$, vortices can also be created in the flow by a 'folding' of the oscillatory motion, trapping fluid that appears in the photographs as stagnant. The stagnant fluid subsequently acquires rotational motion. This pattern has been observed in several sequences of photographs and a typical instance is shown in figure 13 and figure 5 (plate 4), where the arrows point to the developing vortex.

The unexpected result of the present experiment was the persistence of the von Kármán vortices at much greater downstream distances and much higher Reynolds numbers than those previously reported in the literature. The implications of this observation on the mechanism of entrainment of the turbulent wake will be discussed in § 5.

The difference between the present results and those of Roshko (1953) on the persistence of the vortices in the flow can be attributed largely to the irregular and scattered pattern of the vortex street, especially beyond 40 or 50 diameters downstream. The randomization of phasing between vortices could prevent the detection of the periodicity in the street, if a spectral analyser is used, as it was in Roshko's experiments. Another possibility is that periodicity due to the vortex motion in the flow is difficult to detect with a single-sensor probe which responds to changes in the magnitude but not to changes in the orientation of the velocity vector. A sinusoidal variation in the direction of the mean flow has no effect on the output of a single-sensor probe. This was demonstrated by Bevilaqua,† who recorded u and v components of the velocity at the centre-line of the wake of a cylinder using both single and X hot-wire probes at Reynolds numbers 500 and 40000. At this position, the X probe revealed the first harmonic of the shedding frequency. Bevilaqua found that, while the u component of the velocity appeared fully turbulent, the v component showed a pronounced periodicity.

The effect of turbulence in the near wake region will now be discussed. Turbulent action close to the cylinder manifests itself by a sudden broadening of the core of the street at the point indicated by arrows in figures 9, 10 (plates 8, 9).

† Private communication, to be part of a Purdue University doctoral thesis.

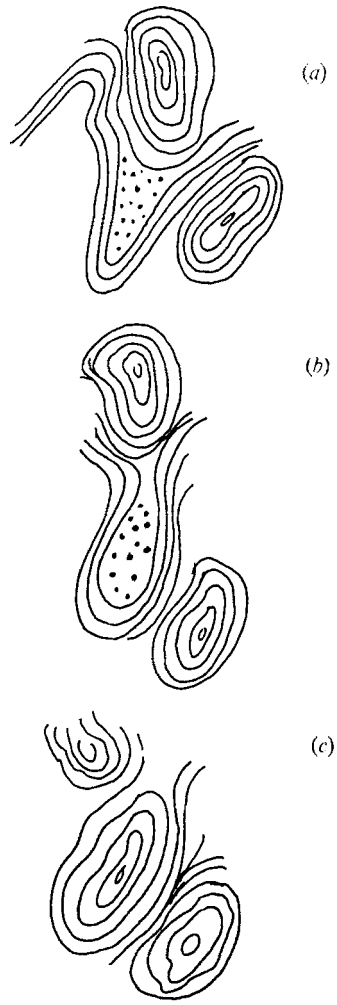

FIGURE 13. Formation of vortices by 'folding' of the oscillatory motion in the wake.

Since transition to turbulence is expected to occur at distances much closer to the cylinder (Schiller & Linke 1933; Bloor 1964) than this point (this was also found in the fully turbulent signals obtained by the hot-film sensor), the location of the sudden broadening should correspond to the position where turbulence becomes strong enough to have an appreciable effect on the street. The broadening of the core coincides with an increase in the longitudinal distance α reported also by Frimberger. As can be seen in the photographs, this location moves closer to the cylinder with increasing Reynolds numbers.

Finally, it can be concluded that the turbulent action produces the initial rapid broadening of the vortex street. As the vortices travel further downstream, they lose their strength owing to the diffusion of vorticity, and this causes their gradual deceleration. The broadening of the vortex street in the downstream direction is shown in figure 4, while figure 5 shows the change of the longitudinal distance α with increasing downstream distances.

4. Theoretical study of the turbulent vortex street

In §4 an attempt will be made to construct a theoretical model which will account for the experimental observations discussed in §3. The motion of the vortex street in turbulent surroundings will be examined. This study will give the change due to the turbulence of the geometrical characteristics of the street h and α in the downstream direction.

As stated in §1, Lin (1954) developed a theory explaining the broadening of the laminar vortex street in the downstream direction due to viscosity. According to his model, the vortex street can be represented by a periodic vorticity perturbation, superimposed on a uniform flow of velocity U. The centres of the vortices, according to his interpretation, correspond to the points of maximum vorticity. Using the Oseen approximation, he derived a two-dimensional vorticity equation to describe the flow. This equation has the form

$$\frac{\partial \omega}{\partial t} + U\frac{\partial \omega}{\partial x} = \nu \nabla^2 \omega, \tag{1}$$

where ω is the vorticity component parallel to the axis of the cylinder, i.e.

$$\omega = \frac{\partial v}{\partial x} - \frac{\partial u}{\partial y}. \tag{2}$$

The relation obtained for the change in the distance h between the two rows of vortices in the downstream direction was of the form

$$h = 2\eta(2\nu x/U)^{\frac{1}{2}}. \tag{3}$$

The similarity parameter η was obtained from a transcendental equation of the form

$$(\eta_0 - \lambda n_0)\cosh \eta_0 \eta = (\eta - \lambda \eta_0)\sinh \eta_0 \eta. \tag{4}$$

The parameter λ was an integration constant which was expected to have a value near unity, while η_0 was given by the relation

$$\eta_0 = \tfrac{1}{2}h_0(U/2\nu x)^{\frac{1}{2}}, \tag{5}$$

in which h_0 was the distance between the two rows of vortices at a point near the origin of the street, where the two rows are parallel. The values of the integration constant λ and the parameter h_0 must be taken from the experiment, reflecting the fact that the mechanism by which the vortices are shed to form the vortex street is not well understood.

A linearized two-dimensional turbulent vorticity equation can be obtained by applying Oseen's method in a flow with velocity components $U+u$ and v. The velocity U is equal to $U_0 - \overline{u}_T$ ($\overline{u}_T$ is the mean translational velocity of the vortices while U_0 is the velocity of the moving cylinder), and u, v are the instantaneous velocity components in the street.

The use of Oseen's perturbation method at high Reynolds numbers can be justified when the velocities $\overline{u}$ and $\overline{v}$ in the wake are very small compared with the velocity U. This assumption is generally valid for wake flows at large distances from the body (far wake region) where the present theory is applied (see e.g. Hinze 1959, chap. 6, p. 380).

We can write for the turbulent flow

$$u = \bar{u} + u', \quad v = \bar{v} + v', \tag{6}$$

where u', v' are the fluctuating parts of the velocity. If we neglect in the averaged linear momentum equations governing the flow in the street terms quadratic in $\bar{u}$, $\bar{v}$ and their derivatives (according to the Oseen approximation), we easily obtain the vorticity equation

$$\frac{\partial \bar{\omega}}{\partial t} + U\frac{\partial \bar{\omega}}{\partial x} + \frac{\partial}{\partial x}\overline{u'\omega'} + \frac{\partial}{\partial y}\overline{v'\omega'} = \nu\nabla^2\bar{\omega}, \tag{7}$$

where $\omega' = (\partial v'/\partial x) - (\partial u'/\partial y)$ is the turbulent component of the vorticity. The terms $\overline{u'\omega'}$ and $\overline{v'\omega'}$ represent turbulent transport of vorticity across planes perpendicular to the x and y directions, respectively.

In a way similar to that introduced by Taylor (1915) in his vorticity transport theory, we can assume that the transport of vorticity in the x and y directions is proportional to the vorticity gradients in these directions. Assuming further that the transport coefficient for vorticity ϵ_ω is a constant, we have that

$$\overline{u'\omega'} = -\epsilon_\omega\frac{\partial \bar{\omega}}{\partial x}, \quad \overline{v'\omega'} = -\epsilon_\omega\frac{\partial \bar{\omega}}{\partial y}, \tag{8}$$

and (7) becomes

$$\frac{\partial \bar{\omega}}{\partial t} + U\frac{\partial \bar{\omega}}{\partial x} = (\nu + \epsilon_\omega)\nabla^2\bar{\omega}. \tag{9}$$

The underlying assumption in the above discussion is that there is no net transport of vorticity across planes perpendicular to the axis of the cylinder, and that on these planes the total amount of vorticity is conserved. This, as is well known, was the main criticism against the vorticity-transport theory, and the reason for its extension by Taylor (1932) to a three-dimensional generalized form. However, in the particular case under consideration, the two-dimensional model sems justifiable to the extent that no appreciable vorticity gradients exist in the z direction. Three-dimensional effects in the vortices, observed very close to the body by many investigators (Hamma 1957; Gerrard 1966*a*; Berger & Wille 1972; Taneda 1965) are not considered in the proposed two-dimensional vorticity-diffusion model. An assessment of their influence on the vortex pattern far downstream is not easy, because these effects and their development in the downstream direction are not adequately known at the present time (see the reviews of Gerrard 1966*a* and Berger & Wille 1972). However, the assumptions of the present model are supported by the observations of Gerrard (1966*a*), who reported that, in the range of Reynolds numbers examined in the present work, the fully turbulent vortices form straight lines parallel to the cylinder. Also, Bloor & Gerrard (1966) found that three-dimensional effects did not significantly change their measurements of two-dimensional vortex strength. Finally, the persistence of vortices observed in the present experiments indicates that the influence of three-dimensional effects on the vortices should be negligible. If these effects had been strong, they would have resulted in a rapid destruction of the vortices. We can therefore assume that the net amount of vorticity trans-

ported across any plane perpendicular to the z direction, owing to the random component w' of the turbulent velocity, is negligible.

The choice of a constant eddy diffusivity for the vorticity can be justified by experimental and theoretical results for the turbulent wake behind bluff bodies in which transport coefficients like those for momentum and heat are constant (Townsend 1949; Wygnanski & Fielder 1970). Also, the use of a constant eddy diffusivity has proved appropriate in the study of turbulent line vortices (Hoffman & Joubert 1963) and vortex streets (Timme 1957, 1958).

As we have seen, the vorticity equation for the two-dimensional turbulent motion (equation (7)) can finally be reduced to the same form as the laminar one (equation (1)). Therefore, the same mathematical method can be applied to define the growth of h due now to the turbulent action expressed by the eddy diffusivity of vorticity ϵ_ω.

The change of h with the distance x is now given by

$$h = 2\eta \left(\frac{2(\nu+\epsilon_\omega)\,x}{U_0}\right)^{\frac{1}{2}}, \tag{10}$$

where η can be obtained from the same transcendental equation (4), in which the eddy diffusivity ϵ_ω has been added to the kinematic viscosity ν. In (10) we replaced U by U_0 on the grounds that, as the experimental measurements showed, $\overline{u}_T$ represents only about 4 % of U_0 in the turbulent flow.

To find an expression for the spacing α of the vortices we may consider that the mean flow in the street, in the range of Reynolds numbers in which the experiments have been conducted, is the same as that of a two-dimensional turbulent wake. The equation of motion in this case is

$$\rho U_0 \frac{\partial \overline{u}}{\partial x} = \epsilon \frac{\partial^2 \overline{u}}{\partial y^2}. \tag{11}$$

If we adopt the same value ϵ_ω for the eddy diffusivity, the solution of (11) gives a Gaussian velocity profile of the form

$$\frac{\overline{u}}{U_0} = A(x/d)^{-\frac{1}{2}} \exp\left\{-\frac{U_0 y^2}{4\epsilon_\omega x}\right\}. \tag{12}$$

The spacing distance α is given by

$$\alpha = \frac{U_0 - \overline{u}_T}{f}, \tag{13}$$

where f is the shedding frequency of the vortices. The increase of α in the downstream direction is due to the decrease of $\overline{u}_T$. We may assume that the velocity $\overline{u}_T$, with which a vortex located at distance x from the cylinder moves, can be obtained from the Gaussian profile (equation (12)) for a value of y equal $\frac{1}{2}h$, the distance of the centre of the vortex from the x axis.

We then obtain

$$\overline{u}_T = AU_0 \left(\frac{x}{d}\right)^{-\frac{1}{2}} \exp\left\{\frac{U_0 h^2}{16\epsilon_\omega x}\right\}; \tag{14}$$

thus the spacing α is given by

$$\alpha = \left(U_0\left[1 - A(x/d)^{-\frac{1}{2}} \exp\left\{-\frac{U_0 h^2}{16\epsilon_\omega x}\right\}\right]\right)\Big/ f. \tag{15}$$

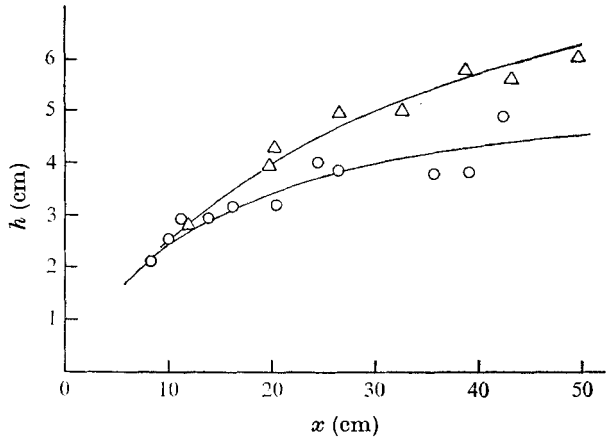

FIGURE 14. Change of distance h in the downstream direction. ——, theory.

	Re	ϵ_ω	λ	d (mm)	
⊙	1080	0·6	0·2	3·175	(160d)
△	5215	2·0	0·2	6·35	(80d)

The origin of self-preservation for the velocity profiles varies with the Reynolds number, and in general lies within a distance of about 80 diameters downstream; yet even at distances closer to the cylinder the velocity profile should not be substantially different from the Gaussian.

The theoretically predicted downstream growth of the vortex street, as obtained from the linearized turbulent vorticity equation with constant eddy diffusivity ϵ_ω (equation (9)), was found to be in good agreement with the experiment (figure 14). The downstream distances covered in this figure correspond to 160 and 80 cylinder diameters for $Re = 1080$ and $Re = 5215$, respectively. The above two cases represent extreme Reynolds numbers for which the theory has been compared with the experiments. The theory has been also compared favourably with experimental results at Reynolds numbers 1730 ($d = 3{\cdot}175$ mm), 2620 ($d = 3{\cdot}175$ mm) and 2650 ($d = 6{\cdot}35$ mm). To the best of the authors' knowledge, there are no similar experiments in the literature for comparison with the present results.

The value 0·2 for the integration parameter λ gives the best fit to the experimental data for all Reynolds numbers studied in the experiments. The eddy diffusivity, chosen as the best fit to the experimental points in the $h = h(x)$ curve, ranged from $\epsilon_\omega = 0{\cdot}6$ for the lowest Reynolds number ($Re = 1080$) to $\epsilon_\omega = 2{\cdot}0$ for the highest one ($Re = 5215$) and it increased continuously with increasing Reynolds number. Because the theory cannot determine the origin of the street, the curves $h = h(x)$ had to be shifted to fit the experimental data† as shown in figure 14.

In a laminar vortex street, Wille & Timme (1957) calculated the relative position of the real and apparent centres of the vortices. Their results, covering the first ten vortices in the street, indicated that the path of the real centres was approximately parallel to that of the apparent centres.

† The same approach was followed by Timme (1958) in his experiments in water.

Bloor & Gerrard (1966) investigated the flow in a turbulent vortex street behind a cylinder. Vortex velocity distributions calculated from measurements obtained within ten diameters behind the cylinder were in good agreement with the velocity distribution described by Hoffman & Joubert (1963) for a turbulent line vortex. This distribution consisted of a turbulent core of radius r_c, outside which the tangential velocity is that of a potential vortex. The velocity in the inner part of the turbulent core, extending to the distance r_1 from the centre at which the maximum velocity fluctuations occur, is proportional to the radius (solid-body rotation). From fluctuating velocity distributions and the location of the centres of the vortices Bloor & Gerrard defined r_1 and r_c at 6 and 10 diameters downstream and at Reynolds numbers 2×10^3 and $1{\cdot}6 \times 10^4$. The radius r_1 was found to increase slightly between the two positions. From these measurements, an approximate value of 4 can be obtained for the ratio r_c/r_1.

If we assume that the diameter of a vortex appearing in the photographs of the present investigation corresponds to the diameter of its turbulent core, and also that there is no significant change of the ratio r_c/r_1 in the downstream direction, we can place the location of the real centres of the vortices closer to the axis of the street, by a distance approximately equal to $\frac{1}{4}r_c$ from the apparent centres.

Estimated values of $r_1 \simeq \frac{1}{4}r_c$ from the photographs, at various Reynolds numbers, ranged between 4 and 6 % of the distance h. Actually, the relative distance between the real and apparent centres should be less than these values since the apparent centres are located within the inner core of the vortices. Accordingly, considering the real centres of the vortices, instead of the apparent ones, would result in a slight lateral shift of the present curve $h = h(x)$ towards the axis of the street, without any appreciable change in its shape. Similar results were found by Wille & Timme in the laminar case. This should be expected, since, in the far wake region where the present measurements were taken (beyond 15–30 diameters downstream), the growth rate of the vortices diminishes. We can conclude that, to obtain the locus $h = h(x)$ of the real centres, a lower value of h_0 than that used for the apparent centres is probably needed, while the parameter λ determining the shape of the curve would be unaltered.

For the theoretical prediction of the variation of the longitudinal distance α far from the cylinder, based on (15), the values of ϵ_ω and h used in the calculation of $\overline{u}_T$ (14) were taken from the theoretical curves $h = h(x)$ for the corresponding Reynolds number. The constant A appearing in (14) was determined from the experimental observation that the velocity $\overline{u}_T$ at 20 diameters downstream was approximately 4 % of the velocity U_0.† Finally, the value of α estimated from (15) at a distance from the cylinder equal to 20 diameters was adjusted to match the experimentally obtained value of α at this point. The change of α with the

† The representative value $\overline{u}_T = 0{\cdot}04\ U_0$ was used in the present calculations, although measured values of $\overline{u}_T$ varied widely (between 3 and 9 % of U_0). This value is less than half of the values generally reported in the literature ($0{\cdot}07 \lesssim \overline{u}_T \lesssim 0{\cdot}25\ U_0$). Except for a slight change in the value of the constant A, a higher value of $\overline{u}_T$ at 20 downstream diameters is not expected to alter the presented results significantly.

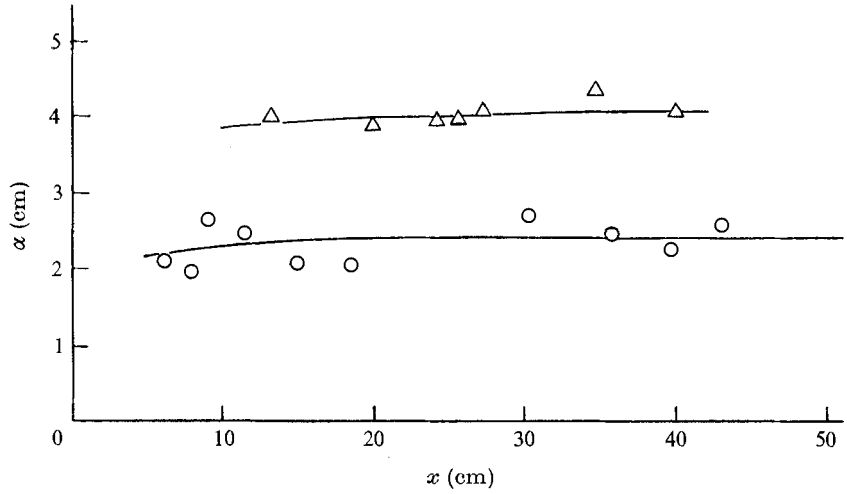

FIGURE 15. Change of longitudinal distance α in the downstream direction. ——, theory.

	Re	ϵ_ω	λ	d (mm)	
⊙	1080	0·6	0·2	3·175	(180d)
△	5215	2·0	0·2	6·35	(90d)

distance x from the cylinder obtained from (15) is in good agreement with the experimental results (figure 15), indicating that the vortex pattern shed by the cylinder is part of the turbulent wake.

5. The entrainment mechanism

The persistence of the vortex structure bears directly on the growth of the wake and the mechanism of entrainment. Corrsin & Kistler (1954) introduced the concept of a 'laminar superlayer' within which the process of entrainment is initiated by viscous shearing forces. Townsend (1966) has described the mechanism as a process of 'nibbling' by the small scale vortices at the surface.

Although these authors recognized the existence of large scale 'billows' and 'convolutions' at the surface, the significance of vortices in determining the form of the interface was first recognized by Bevilaqua & Lykoudis (1971). They studied the mechanism of entrainment in the turbulent wake of a sphere. From observations of the way in which dyed droplets of fluid were absorbed by the growing wake, they concluded that the rotation of large vortices associated with surface waves was responsible for the bulk of the entrainment.

The present work supports the hypothesis of Bevilaqua & Lykoudis. It also clarifies the question of the origin of the vortices in the wake. In the photographs, the vortices shed by the cylinder are seen to form a turbulent vortex street which persists far downstream. On the basis of this observation, the entrainment process can be interpreted as follows.† The origin of the surface convolutions is the vortices of the turbulent vortex street. A vortex draws fluid from the region outside the street into the wake as it rotates, by the action of turbulent shearing

† A more complete discussion is given by Bevilaqua. See footnote, p. 21.

forces. Part of the fluid entrained remains within the vortices, leading to their growth, while the remainder diffuses into the turbulent core by the action of the turbulence. Evidence that entrained fluid finds its way into the core can be found in the present photographs, in which it can be seen that the core as well as the vortices themselves grow in the downstream direction. Accordingly, the entrainment mechanism can be thought of as a 'pumping' process which brings fluid into the wake. Because of the turbulent nature of the vortex motion, the amount of fluid entrained is considerably larger than that corresponding to a purely viscous laminar vortex street, in which case the growth is due to viscous diffusion of the vortices.

The widening of the turbulent vortices and the core is very rapid in the near wake, indicating strong entrainment in this region. As the vortices move downstream, they are diffused by the action of the turbulence, and thus lose their strength, so that the rate of entrainment is slowed. However, entrainment never stops completely, as indicated by the continuing increase of h in the downstream direction (figure 14). There is a loss of order in the vortex street at distances far downstream. It is possible that the point where the street does break up and the vortices decay completely coincides with the beginning of similarity as reported by Townsend.

It should be noted that the experimental evidence presented by previous investigators does not contradict the results of the present work. Townsend (1966) reported the existence of periodicity in the flow associated with his surface waves, and described a growth and decay cycle with an associated variation in the rate of entrainment. Grant (1958) observed a similar periodicity in the wake of a cylinder. Grant (1958, figure 11), in particular, suggests the existence of vortices at the interface.

Keffer (1965) observed that the turbulent wake of a cylinder could be reduced to a von Kármán-like double row of vortices when it was strained along the axis of the cylinder. This is probably due to the amplification of the already existing vortex pattern observed in the present work. Oswald & Kibens (1971) studied the structure of the 'bulges' in the far wake of a disk. Using the method of conditioned sampling, which produces flow averages conditioned to the presence or absence of turbulence, they mapped the velocity field about an average bulge. They concluded that the dominant mechanism of entrainment was the nibbling process proposed by Townsend, but also reported that these bulges were observed to 'swirl' with respect to an observer moving with their mean convection velocity. It is likely these bulges represent vortices in the final stages of decay. Even in the axisymmetric case, then, it appears that vortices are responsible for the growth of the wake.

The authors are grateful to Mr P. Bevilaqua for constructive discussions on the entrainment mechanism, and to the reviewers of this paper for their valuable comments. The financial support of the National Science Foundation (grant GK-23694) is also gratefully acknowledged.

REFERENCES

BERGER, E. 1964*a* *Z. Flugwiss.* **12**, 41.

BERGER, E. 1964*b* *Jahrbuch. WGLR*, p. 164.

BERGER, E. & WILLE, R. 1972 *Ann. Rev. Fluid Mech.* **4**, 313.

BEVILAQUA, P. M. & LYKOUDIS, P. S. 1971 *A.I.A.A. J.* **9**, 1657.

BIRKHOFF, G. 1952 *Proc. Natn. Acad. Sci. U.S.A.* **38**, 409.

BIRKHOFF, G. & ZARANTANELLO, E. H. 1957 *Jets, Wakes and Cavities.* Academic.

BLOOR, M. S. 1964 *J. Fluid Mech.* **19**, 290.

BLOOR, M. S. & GERRARD, J. H. 1966 *Proc. Roy. Soc.* A **294**, 319.

CORRSIN, S. & KISTLER, A. L. 1954 *N.A.C.A. Tech. Note*, no. 3133.

DOMM, V. 1955 *J. Aero. Sci.* **22**, 750.

DOMM, V. 1956 *Z. agnew. Math. Mech.* **36**, 367.

FRIMBERGER, R. 1957 *Z. Flugwiss.* **5**, 355.

GASTER, M. 1969 *J. Fluid Mech.* **38**, 565.

GASTER, M. 1971 *J. Fluid Mech.* **46**, 749.

GERRARD, J. H. 1961 *J. Fluid Mech.* **11**, 244.

GERRARD, J. H. 1965 *J. Fluid Mech.* **22**, 187.

GERRARD, J. H. 1966*a* *J. Fluid Mech.* **25**, 143.

GERRARD, J. H. 1966*b* *J. Fluid Mech.* **25**, 401.

GERRARD, J. H. 1967 *Phil. Trans.* A **261**, 137.

GRANT, H. L. 1958 *J. Fluid Mech.* **4**, 149.

HAMMA, F. R. 1957 *J. Aero. Sci.* **24**, 156.

HINZE, J. O. 1959 *Turbulence.* McGraw-Hill.

HOFFMAN, E. R. & JOUBERT, P. N. 1963 *J. Fluid Mech.* **16**, 395.

HOOKER, S. G. 1936 *Proc. Roy. Soc.* A **154**, 67.

HUMPHREYS J. S. 1960 *J. Fluid Mech.* **9**, 603.

JONES. G. W., CINCOTTA, J. J. & WALKER, R. W. 1969 *N.A.S.A. Tech. Rep.* R 300.

KEEFE, R. T. 1961 *UTIA Rep.* no. 76.

KEFFER, J. F. 1965 *J. Fluid Mech.* **22**, 135.

KOVASZNAY, L. S. G. 1949 *Proc. Roy. Soc* A **198**, 174.

LIN, C. C. 1954 *Studies etc. Presented to R. von Mises*, p. 170. Academic.

MARRIS, A. W. 1964 *J. Basic Eng.* **10**, 185.

MATTINGLY, G. E. 1962 *University of Maryland Tech. Note*, BN295.

MORKOVIN, M. V. 1964 Flow around circular cylinder: a kaleidoscope of challenging fluid phenomena. *ASME Fluids Eng. Div. Conf. Symp. on Fully Separated Flows.* A.S.M.E.

OSWALD, L. J. & KIBENS, V. 1971 *Department of Aerospace Engineering, University of Michigan Tech. Rep.* no. 2820.

ROSENHEAD, L. 1953 *Adv. in Appl. Mech.* **3**, 185.

ROSHKO, A. 1953 *N.A.C.A. Tech. Note*, no. 2913.

ROSHKO, A. 1954 *N.A.C.A. Tech. Note*, no. 3169.

ROSHKO, A. 1961 *J. Fluid Mech.* **10**, 354.

SCHILLER, L. & LINKE, W. 1933 *Z. Flugtech. Motorluft*, **24**, 193.

SHAIR, F. H., GROVE, A. S., PETERSEN, E. E. & ACRIVOS, A. 1963 *J. Fluid Mech.* **17**, 546.

STROUHAL, V. 1878 *Ann. Phys. Chem.* **5**, 216.

TANEDA, S. 1955 *J. Phys. Soc. Japan*, **11**, 302.

TANEDA, S. 1959 *J. Phys. Soc. Japan*, **14**, 843.

TANEDA, S. 1965 *J. Phys. Soc. Japan*, **20**, 1714.

TAYLOR, G. I. 1915 *Phil. Trans.* A **215**, 1.

TAYLOR, G. I. 1932 *Proc. Roy. Soc.* A **135**, 685.

TIMME, A. 1957 *Ing. Arch.* **25**, 205.

TIMME, A. 1958 *DVL Bericht*, no. 77.

TOWNSEND, A. A. 1949 *Proc. Roy. Soc.* A **197**, 124.

TOWNSEND, A. A. 1956 *The Structure of Turbulent Shear Flow.* Cambridge University Press.

TOWNSEND, A. A. 1966 *J. Fluid Mech.* **26**, 689.

TRITTON, D. J. 1959 *J. Fluid Mech.* **6**, 547.

TRITTON, D. J. 1971 *J. Fluid Mech.* **45**, 203.

VON KÁRMÁN, T. & RUBACH, H. 1912 *Physic*, A **13**, 49.

WILLE, R. 1960 *Adv. Appl. Mech.* **6**, 273.

WILLE, R. 1966 *Progress in Aeronautical Science*, vol. 7, p. 195. Pergamon.

WILLE, R. & TIMME, A. 1957 *Jahrbuch der Schiffbautechn. Gesellschaft*, **51**, 215.

WYGNANSKI, I. & FIELDER, H. E. 1970 *Boeing Scientific Research Laboratories*, D1 82 0951.

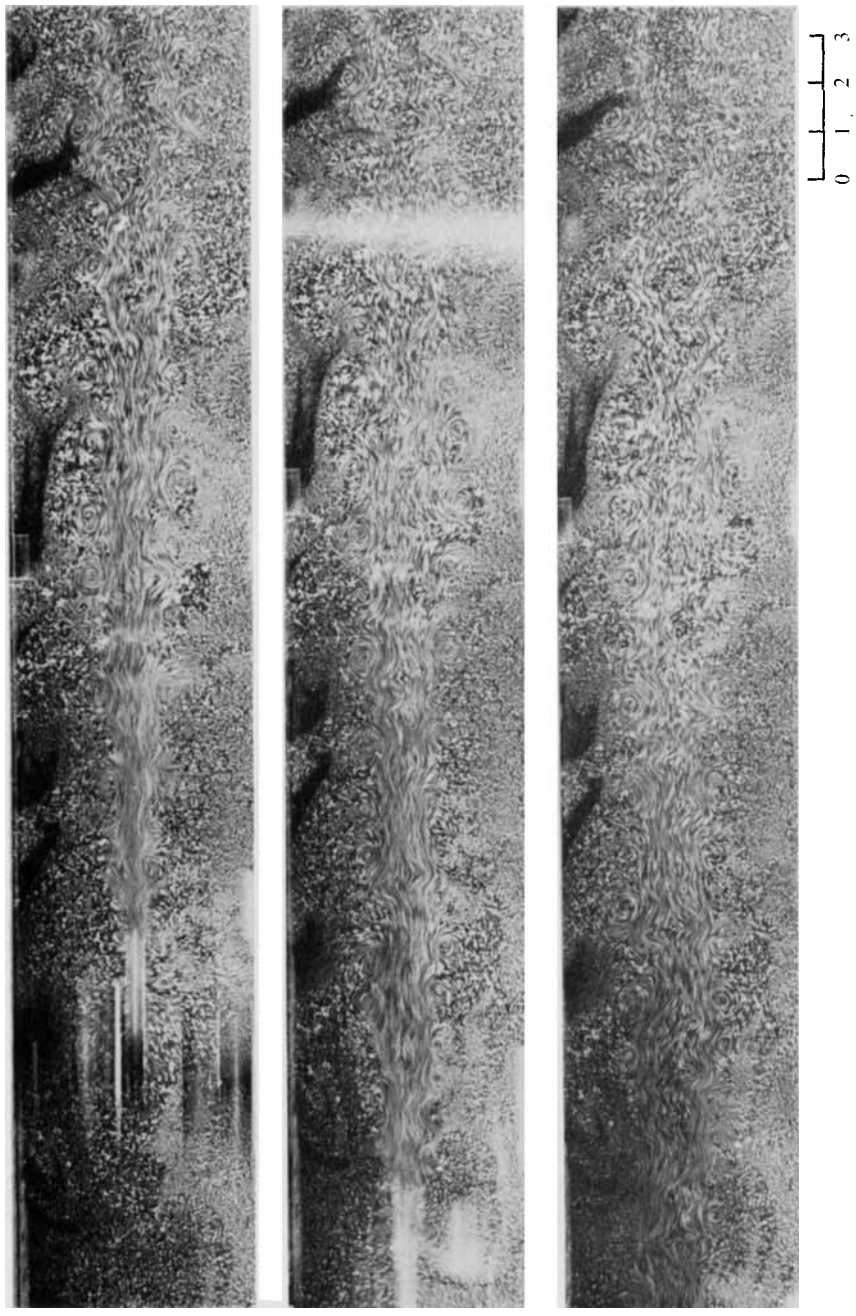

FIGURE 2. Vortices travelling at the edges of a turbulent core. ($Re = 1730$, $d = 3{\cdot}17$ mm, $U_0 = 6{\cdot}35$ cm s^{-1}, exposure time 1 s, 1 picture per 2 s. Downstream distance covered: ~ 300 diameters.)

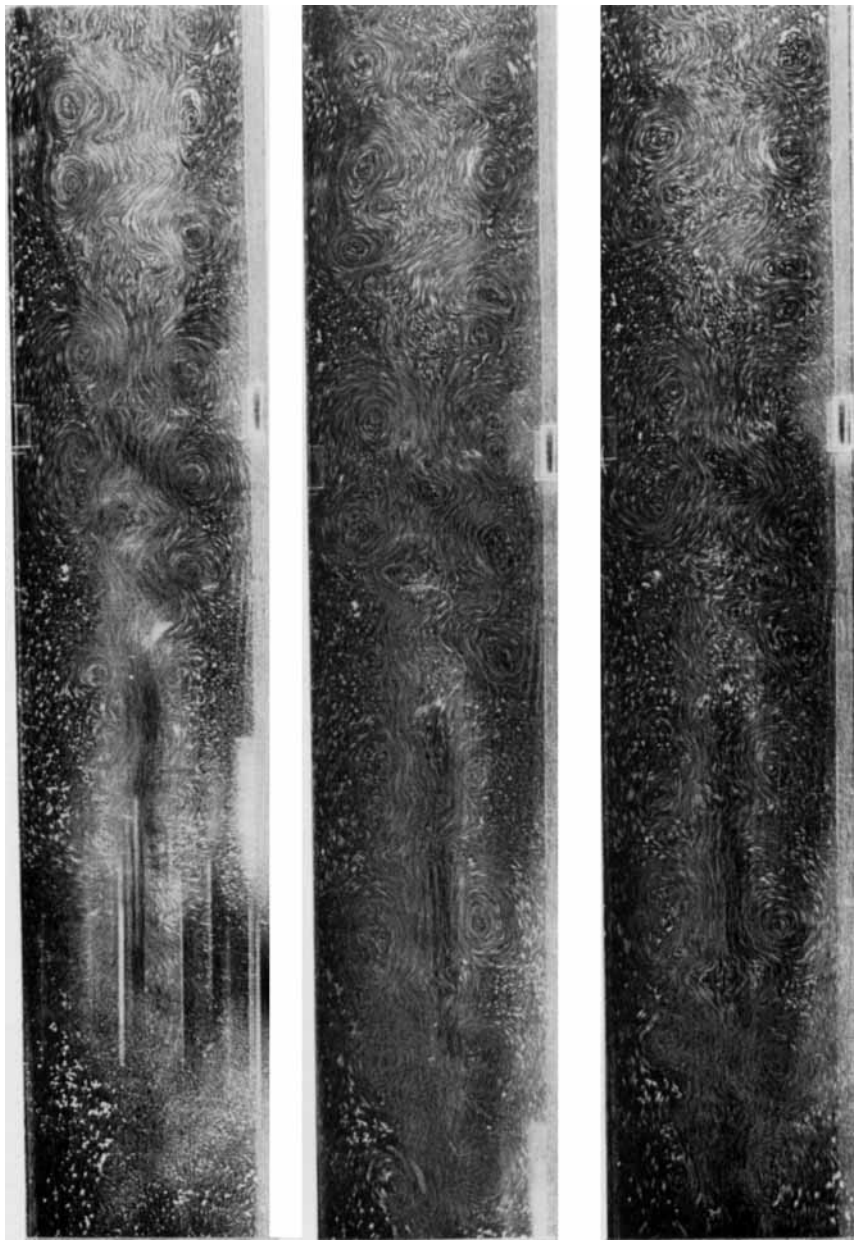

FIGURE 3. Vortices travelling at the edges of a turbulent core. ($Re = 5215$, $d = 6{\cdot}35$ mm, $U_0 = 9{\cdot}42$ cm s^{-1}, exposure time 1 s, 1 picture per 2 s. Downstream distance covered: $\sim$ 180 diameters.)

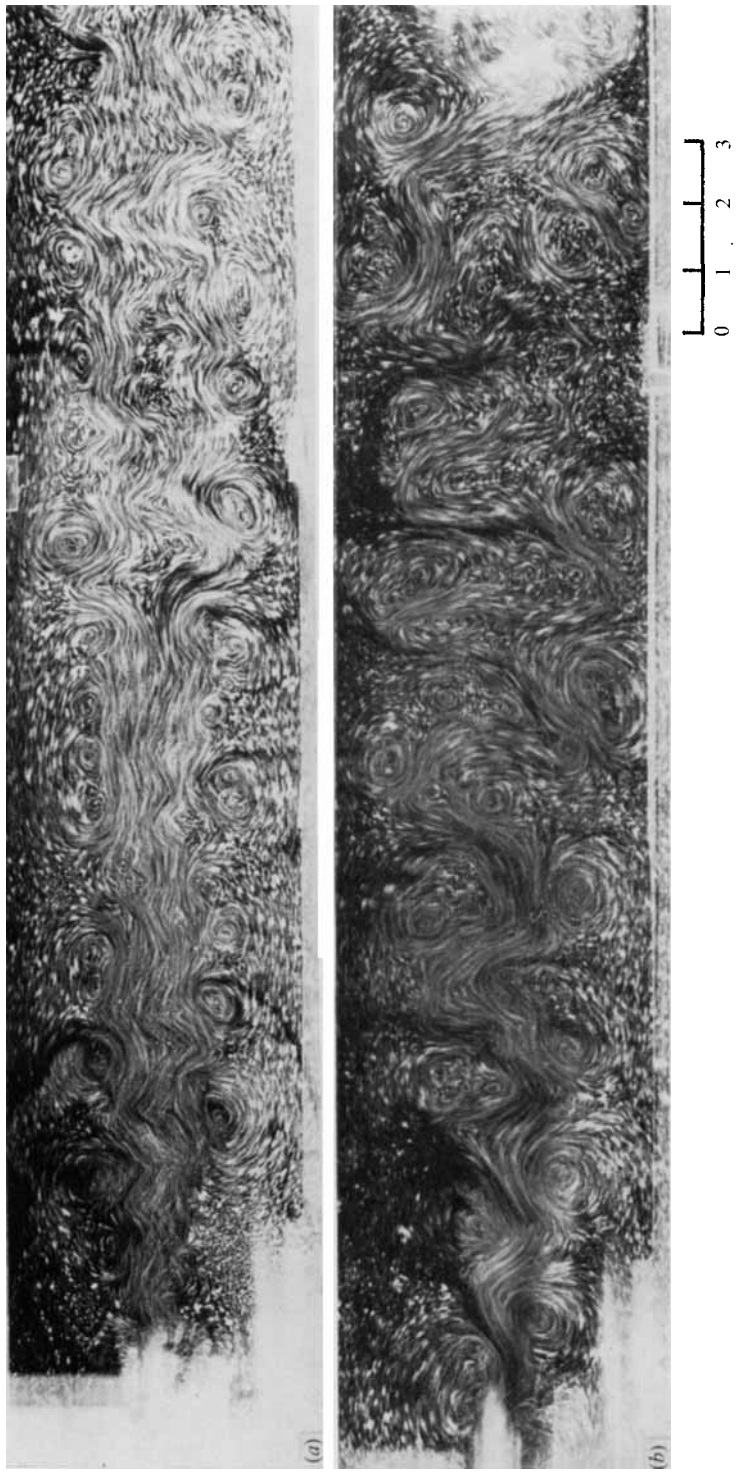

FIGURE 4. Change in the structure of the wake at about $Re = 5500$.

	Re	*d* (mm)	U_0 (cm s^{-1})	Exposure time (s)
(*a*)	5480	6·35	9·92	1
(*b*)	5850	9·53	7·06	1

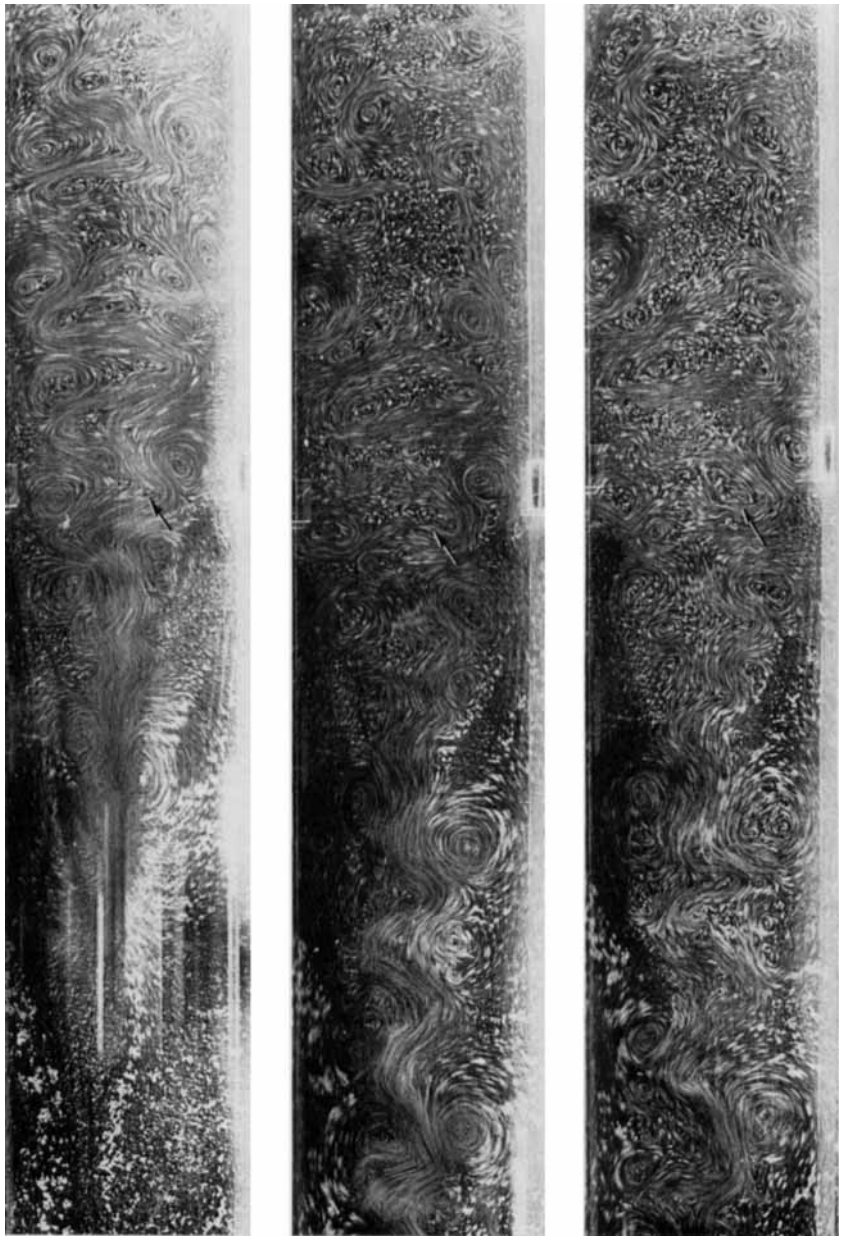

FIGURE 5. Structure of the wake at $Re = 13\,000$, $d = 16$ mm, $U_0 = 9{\cdot}42$ cm s^{-1}, exposure time 1 s, 1 picture per 2 s. Downstream distance covered: ~ 80 diameters.

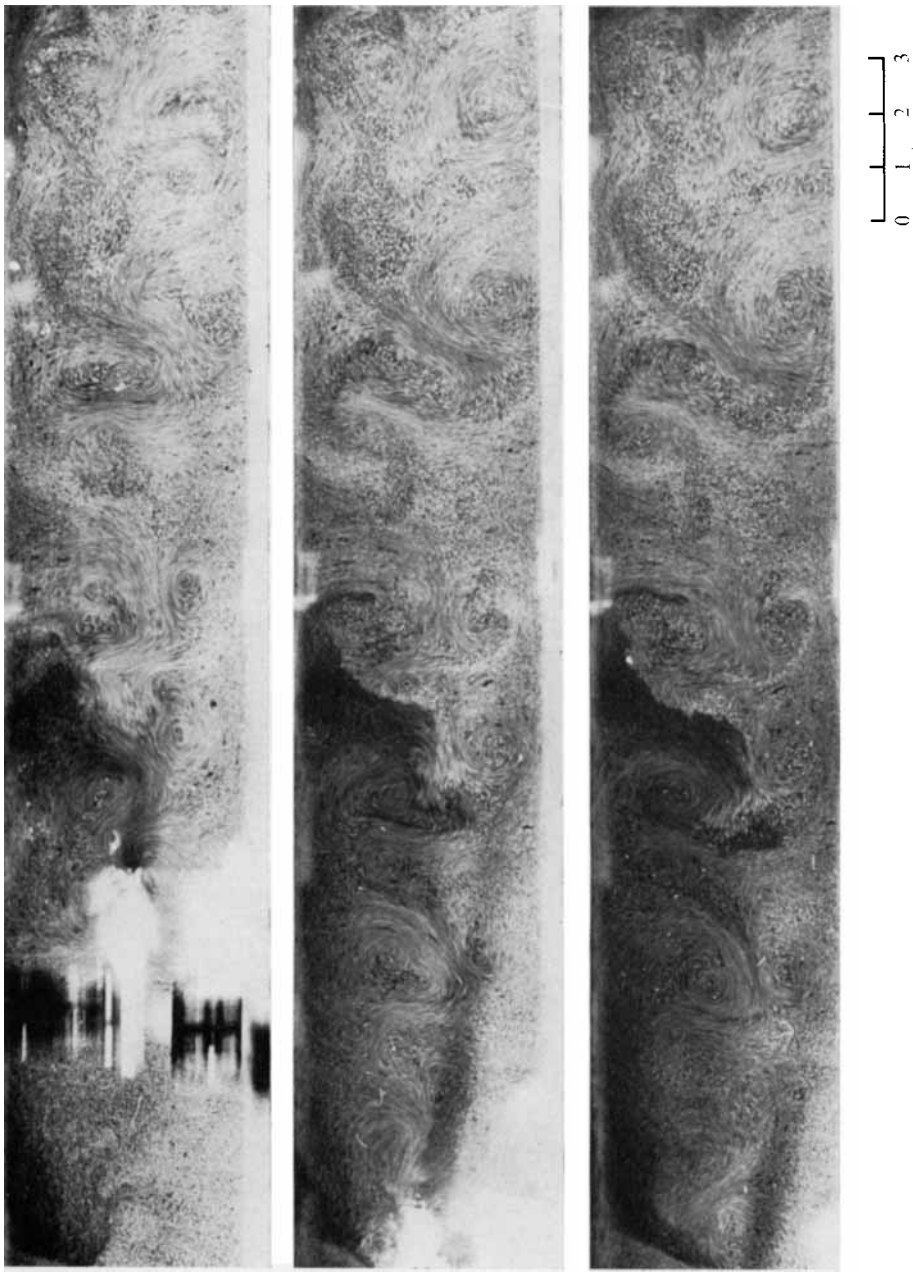

FIGURE 6. Structure of the wake at $Re = 18200$, $d = 16$ mm, $U_0 = 14{\cdot}5$ cm s^{-1}, exposure time 0·125 s, 2 pictures per 1 s. Downstream distance covered: ~ 60 diameters.

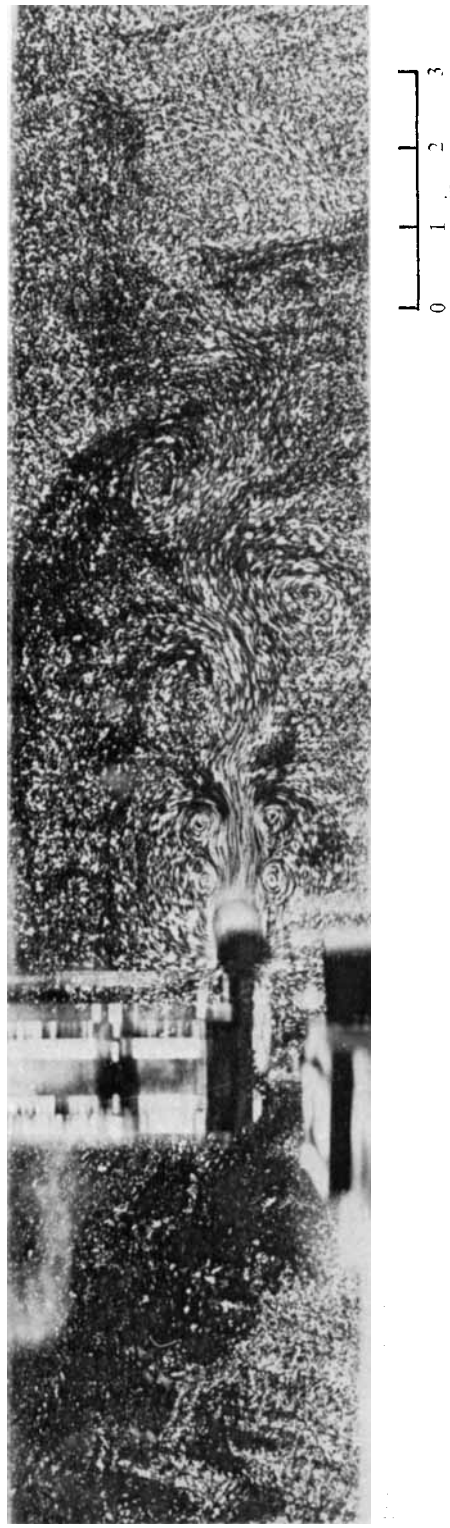

FIGURE 7. Secondary vortices and the formation of a double vortex sheet instability. $Re = 3400$, $d = 16$ mm, $U_0 = 2{\cdot}46$ cm s^{-1}, exposure time 0·25 s. Observation starts at 0·4 diameters downstream.

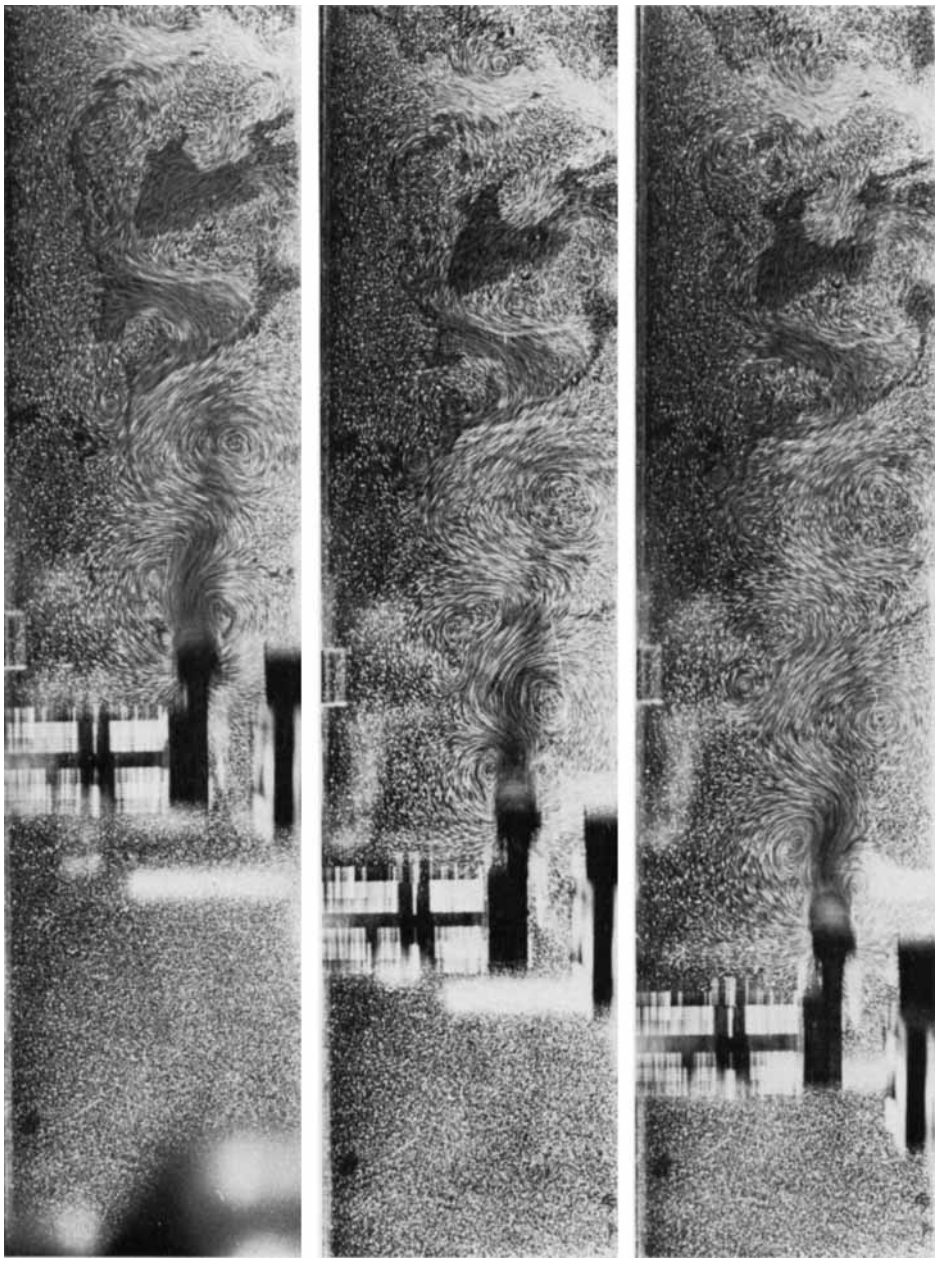

FIGURE 8. Secondary vortices and the formation of a double vortex sheet instability. $Re = 19500$, $d = 16$ mm, $U_0 = 14{\cdot}11$ cm s^{-1}, exposure time 0·25 s, 1 picture per 1 s. Observation starts at 2·2 diameters downstream.

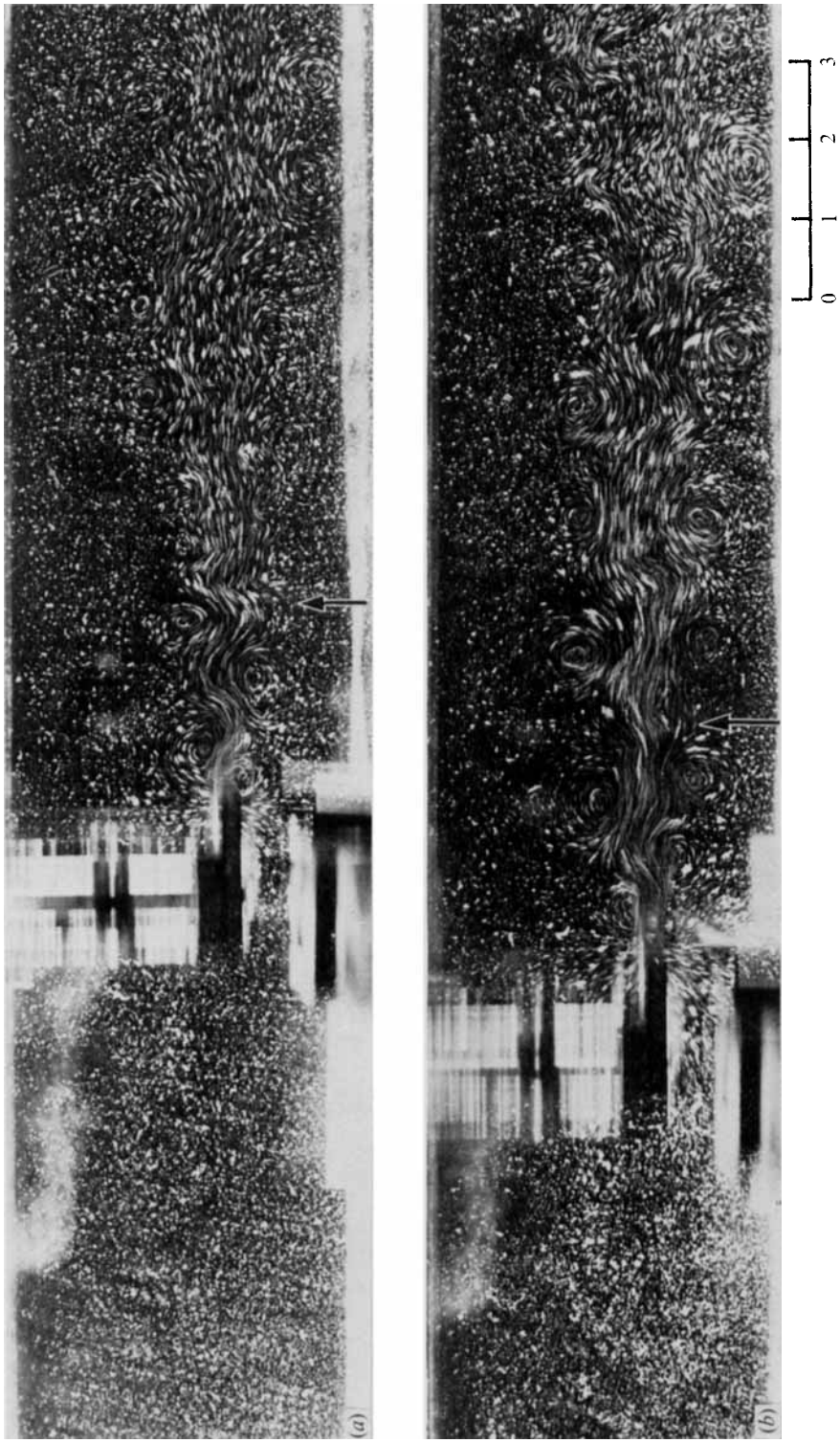

FIGURE 9. The double vortex sheet instability and the appearance of transition to turbulence.

	Re	*d* (mm)	U_0 (cm s^{-1})	Exposure time (s)
(*a*)	2830	6·35	5·11	0·25
(*b*)	4480	6·35	8·11	0·25

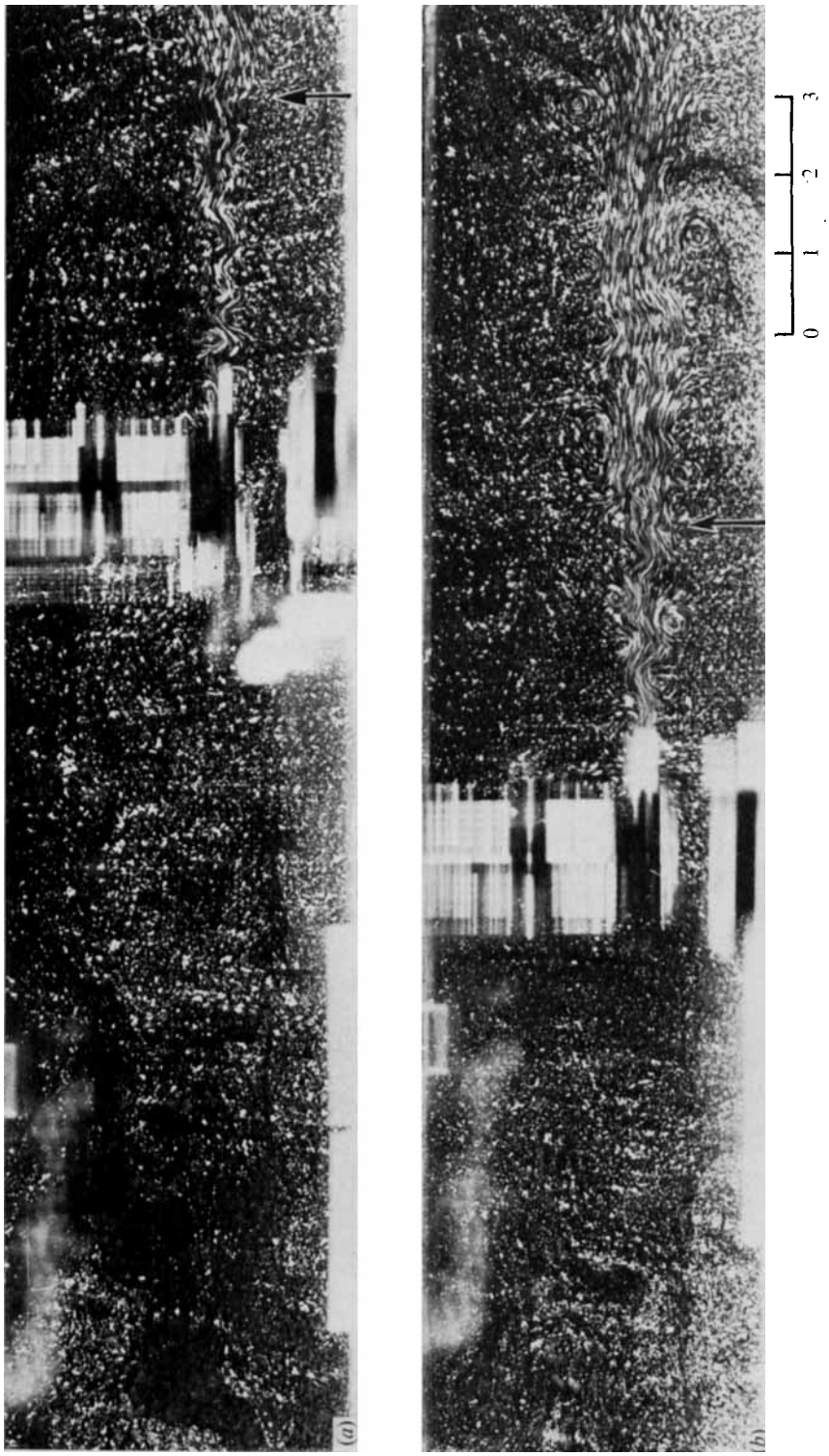

FIGURE 10. Transition to turbulence.

	Re	*d* (mm)	U_0 (cm s^{-1})	Exposure time (s)
(*a*)	1410	3·17	5·11	0·25
(*b*)	2240	3·17	8·11	0·25

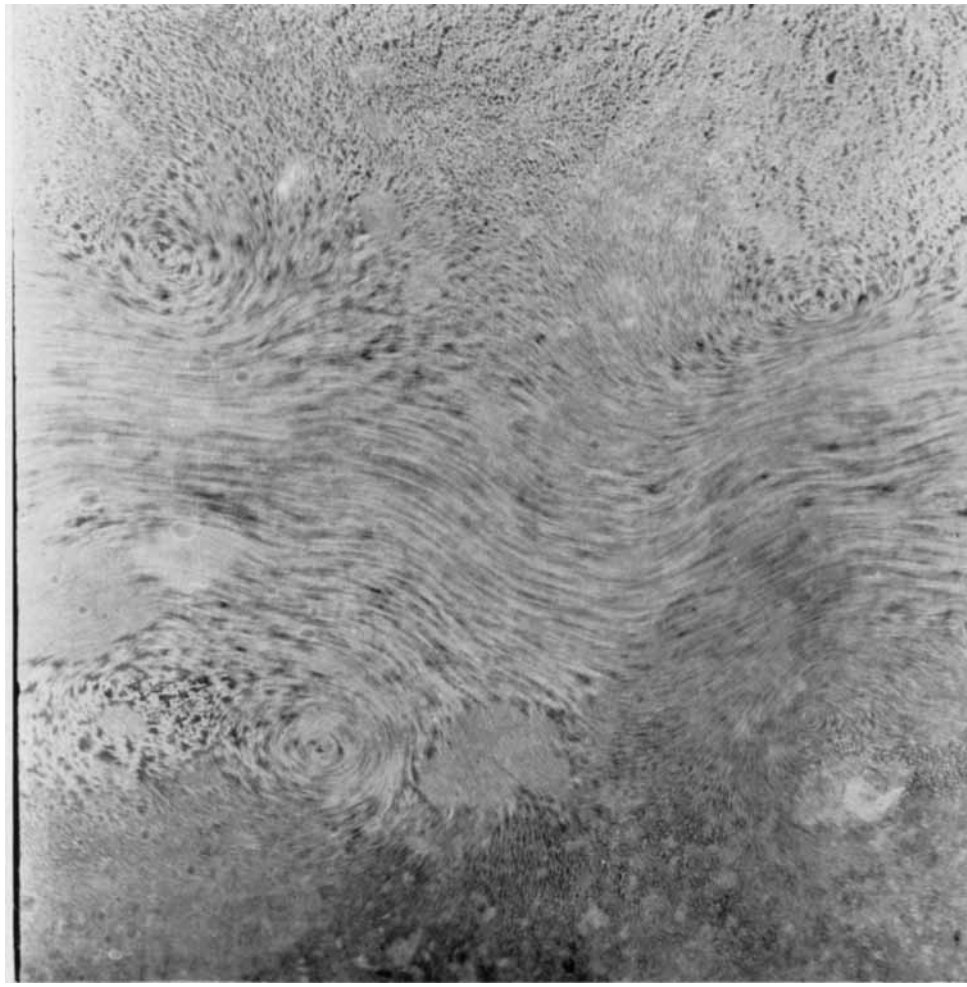

FIGURE 11. Wake structure at a distance $460d$ downstream from a cylinder moving in water.